

# Electrodeposition and characterization of amorphous Cr-P alloys

B. A. DENEVE, S. B. LALVANI\*

*Mechanical Engineering and Energy Processes, Southern Illinois University at Carbondale, Carbondale, IL 62901, USA*

Received 27 September 1990; revised 9 July 1991

The influence of plating variables and bath composition on electrodeposition of chromium-phosphorous alloy composition was investigated. The plating bath, prepared at a pH of approximately 1.25, consisted of a trivalent chromium source, sodium hypophosphite, ammonium sulphate, boric and formic acids, and sodium lauryl sulphate. Energy dispersive spectroscopy and Auger electron spectroscopy were utilized to evaluate alloy composition. These alloys were determined to be amorphous by X-ray diffraction. The influence of temperature, and bath ageing, and deposition time on deposit composition and structure and the deposition rate were also investigated.

## 1. Introduction

An amorphous material lacks the long range atomic order characteristic of a crystalline material; only short-range order exists over a few atomic distances. An amorphous material possesses properties which are unique to its structure. Amorphous alloys, also referred to as metallic glasses, have hardness properties similar to silicate glass, but the toughness properties similar to metals [1]. Amorphous materials also possess unique electrical and magnetic properties. They typically are one of the easiest materials to magnetize and demagnetize, qualifying them as very good soft ferromagnets.

One of the most widely used engineering coatings is the conventional chromium electrodeposit. It provides a high degree of wear resistance, readily forms a protective oxide film and is esthetically pleasing. Conventional chromium is commonly plated from a bath developed by Sargent [2]. Typical chromium deposits contain a large number of microcracks which are induced by stress relieving during the plating process [3]. Hoare [4] recently proposed a mechanism by which chromium is plated from the Sargent bath, which contains chromic oxide ( $\text{CrO}_3$ ) and sulphuric acid in a weight ratio of 100:1. The use of the hexavalent chromium plating bath for chromium deposition has been wide-spread, but this bath has many technical, environmental and health related disadvantages [5].

Modifications to the Sargent bath have been made by various investigators to improve the coating quality as well as the plating process. Yoshida [6] and Ishaguro [7] were probably the first investigators to develop a useful trivalent bath for chromium deposition. A review of the developments in trivalent chromium plating prior to 1975 is provided by Crowther and Renton [8]. Hoshino *et al.* [9] included an organic

additive with a -CHO or a -COOH group to a chromic acid bath. They found the inclusion of these additives effective in producing an amorphous carbon-containing chromium coating. X-ray photoelectron spectroscopy (XPS) and Auger electron spectroscopy (AES) analyses of these coatings were reported by Hoflund, *et al.* [10, 11]. Similar chromium coatings from chromic acid baths containing organic additives have been developed by Dash and Kasaaian [12], Benaben [13] and Furuya *et al.* [14].

Chromium coatings have also been deposited from baths which contain only trivalent chromium ions [15-17]. All of the baths contain an organic additive which prevents the hydrolysis of the chromium ion. Those prepared by Willis and Hammond [17] had an amorphous structure. An electroplated chromium-phosphorus alloy was studied by Bondar and Potapov [18] with no organic additive included in the bath. Watson and coworkers [19-21] have demonstrated sustained deposition of chromium, and its alloys from Cr(III) baths through control of transient Cr(II). They have shown that the transient Cr(II) catalyses interfering oxidation reactions in the diffusion layer which at the pH values, about 4, found in the diffusion layer would otherwise occur too slowly to be significant.

The addition of phosphorus to a chromium-based coating has a two-fold purpose. First of all, being a metalloid it should aid the formation of an amorphous structure during the electrodeposition process. Secondly, the addition of a metalloid should enhance the corrosion properties of the alloy. Moffat *et al.* [22] have determined the superior corrosion resistant properties of a r.f.-sputtered Cr-P alloy.

This work is an investigation of the electrodeposition of amorphous Cr-P-C alloys from a trivalent chromium plating bath. The effect of bath composition and plating variables on the composition of the alloy was studied. An organic additive was included in

\* To whom all correspondence should be addressed.

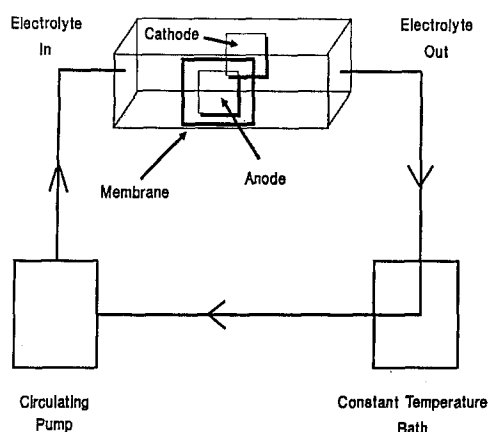


Fig. 1. A schematic sketch of electrodeposition system.

the plating bath as a trivalent chromium complexant. By using this component, carbon is introduced into the alloy. Carbon is also a metalloid and is known to aid in the formation of an amorphous structure.

## 2. Experimental procedure

### 2.1. Electrodeposition

The electrolyte was prepared with distilled water and reagent grade chemicals. The organic complexant was added to the solution a minimum of one hour prior to plating. The pH adjustments were made by adding either NaOH or H<sub>2</sub>SO<sub>4</sub> to the electrolyte. Nitrogen was bubbled through the electrolyte for 10 min prior to deposition. The copper substrate used was a 25 μm thick foil (99.999% purity). Electrodeposition was performed under constant current conditions.

A diagram of the plating system is given in Fig. 1. The electrolyte was pumped through the plating cell to ensure thorough agitation at a rate of 1.5 dm<sup>3</sup> min<sup>-1</sup>. The anode and cathode were placed parallel to each other, 3.2 cm apart. The area of the cathode was 4 cm<sup>2</sup>. A 6.5 cm<sup>2</sup> platinum anode was utilized. The anode and cathode were separated by a DuPont Nafion™ ion selective membrane, thus preventing Cr<sup>6+</sup>, which is an oxidation product of Cr<sup>3+</sup> from passing to the cathode. The electrolyte temperature was maintained within ± 2° C of the desired temperature by a water-jacketed reservoir.

The faradaic efficiencies were calculated with compositional information obtained by energy dispersive X-ray analysis (EDX). The equipment available for this analysis does not detect carbon, so efficiency calculations were based on chromium and phosphorus compositions only.

### 2.2. Cyclic voltammetry

The electrolyte was prepared in the same manner as the electrodeposition solution. Nitrogen was purged through the electrolyte approximately 10 min prior to testing. The programmable potentiostat used for performing cyclic voltammetry was the BioAnalytical System Model 100. A three-electrode cell containing a platinum wire for the counter electrode, a glassy

Table 1. Plating bath for chromium-phosphorous-carbon electro-deposition

Component	Concentration/g dm <sup>-3</sup>
Cr <sub>2</sub> (SO <sub>4</sub> ) <sub>3</sub> · nH <sub>2</sub> O (20% Cr)	180
NaH <sub>2</sub> PO <sub>3</sub> · H <sub>2</sub> O	0-30
(NH <sub>4</sub> ) <sub>2</sub> SO <sub>4</sub>	100
H <sub>3</sub> BO <sub>3</sub>	50
NH <sub>4</sub> Br	10
HCOOH	20
(CH <sub>3</sub> (CH <sub>2</sub> ) <sub>10</sub> CH <sub>2</sub> OSO <sub>3</sub> Na)	0.1
pH ≈ 1.25	

carbon micro-electrode (diameter 3.2 mm) for the working electrode, and a Ag/AgCl reference electrode were utilized.

### 2.3. Composition and structure

The alloy composition was determined by Energy dispersive X-ray diffraction analysis (EDX) and Auger electron spectroscopy (AES). The surface was cleaned with acetone prior to analysis. The alloy was sputtered to a depth of 20 nm for AES.

The structure of the alloys was determined by X-ray diffraction (XRD). Diffraction was performed in a 2θ range of 5° to 144°.

## 3. Results and discussion

### 3.1. Electrodeposition studies

Chromium-phosphorus-carbon alloys were plated from the bath listed in Table 1. Chromium sulphate was the trivalent chromium source. Sodium hypophosphite was included as the phosphorus source. Ammonium sulphate is a complexant possibly in the high pH of the diffusion layer. Boric acid (pK 9) served as a source of a borate complex at the pH values involved. The chief acid/base buffer in the electrolyte is the aquo-chromium (III) ion (pK ≈ 4). Also included in the bath were ammonium bromide, an anti-oxidant; formic acid, the trivalent chromium complexant; and sodium lauryl sulphate, the wetting agent. The bath was operated at a pH of approximately 1.2-1.3. In the experiments described below, a Nafion™ membrane was used to isolate the working electrode compartment. Thin films of very poor quality were obtained when the membrane separator was not employed.

### 3.2. Effect of bath composition

The effect of bath composition on alloy composition was studied by varying the sodium hypophosphite concentration from 0 to 30 g dm<sup>-3</sup>, while the chromium sulphate concentration was maintained at 180 g dm<sup>-3</sup>. Figure 2 contains results from depositions performed at 20 A dm<sup>-2</sup> and 30° C. The phosphorus composition of these alloys, as determined by EDX, was found to increase with the phosphorus content of the plating bath. There is a nearly linear relationship

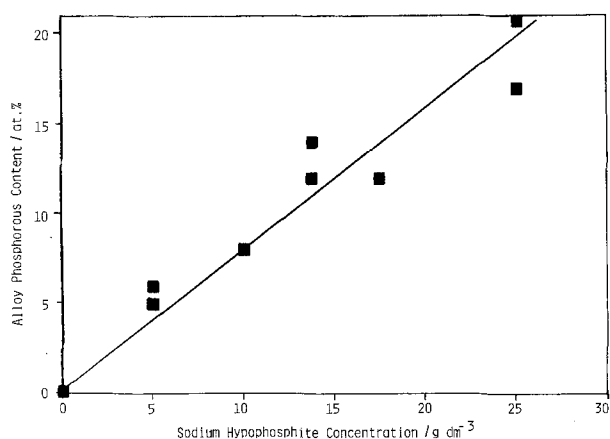


Fig. 2. Alloy phosphorus content against phosphorus in bath. Experiments were conducted at  $20 \text{ A dm}^{-2}$  and  $30^\circ \text{C}$ . The bath composition as in Table 1.

between the amount of phosphorus in the bath and the phosphorus content of the alloy.

The composition of the Cr-21 at % P-C sample was further analysed by AES to determine carbon and oxygen contents. The AES profile is shown in Fig. 3. The sample which was estimated to contain 21 at % P (by EDX) was found to consist of 28 at % P, 8 at % O, and 7 at % C by AES at a sputter depth of 20 nm. The differences in P content can be accounted for by the fact that EDX measures bulk composition, whereas AES is only a surface analysis and also detects the lower atomic weight elements. The discrepancy can also be attributed to the accuracy of the AES system, with a maximum uncertainty in measurement of up to 50 at %, depending on the element analysed. This alloy also contained impurity levels of sulphur, which were not quantified.

Alloys were also prepared with the plating bath stated in Table 1, except that the bath contained no sodium hypophosphite. The Cr-C coatings produced from the bath were bright in appearance. EDX analysis showed 99 at % chromium, while AES analysis indicated 75 at % Cr, 7 at % O, and 18 at % C at a sputter depth of 20 nm for this alloy. These results indicate that under identical reaction conditions, the overall metalloid (i.e. P + C) concentration is much greater for baths that contain a mixture of sodium

hypophosphite and formic acid than for those containing formic acid only.

### 3.3. Effect of temperature

Alloys were deposited at 30, 35, 40, and  $50^\circ \text{C}$  to determine the effect of temperature on the alloy composition. Experiments were conducted at constant current density of  $20 \text{ A dm}^{-2}$  using the bath composition shown in Table 1 ( $15 \text{ g dm}^{-3} \text{ NaH}_2\text{PO}_2$ ). The results are shown in Fig. 4. A monotonic linear relationship between the alloy phosphorous content and the bath temperature is observed. Since phosphorus deposition from thermodynamic considerations should take place at potentials more positive than chromium deposition, an increase in temperature is expected to favour phosphorus deposition as its deposition is anticipated to be mass transport limited as compared to chromium deposition. The data obtained support this hypothesis.

### 3.4. Effect of current density

The influence of the applied current density on the composition of the Cr-P-C alloys was also investigated. At the lowest applied current density used in this work,  $10 \text{ A dm}^{-2}$ , no coating could be attained. At the low current density, the cathode potential is probably too noble to induce deposition of chromium.

At a current density of  $15 \text{ A dm}^{-2}$ , coatings could be obtained, but they were very thin, approximately  $1 \mu\text{m}$ , with incomplete coverage of the substrate. These coatings could be easily scraped off the substrate. Evidently, the rate of chromium reduction is very small at the applied current density of  $15 \text{ A dm}^{-2}$ . Also very low cathodic efficiencies (less than 2.5%) were observed. The phosphorus content of the two alloys obtained were 15 and 19 at % (by EDX) with a sodium hypophosphite concentration of 5 and  $10 \text{ g dm}^{-3}$ , respectively (Fig. 5).

At a current density of  $20 \text{ A dm}^{-2}$ , the physical appearance of the coatings ranged from 'matted' to 'bright'. The phosphorus content of these alloys varied from 6 to 21 at % (by EDX), and were discussed previously. The plating efficiencies of these coatings ranged from 6–16%, however they bear no

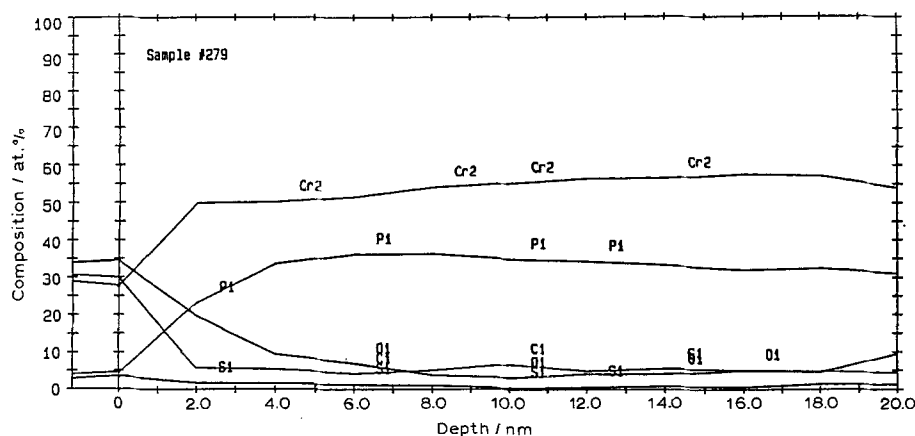


Fig. 3. Auger depth profile of chromium-phosphorus-carbon alloy. The alloy was produced from the bath shown in Table 1 at  $20 \text{ A dm}^{-2}$  and  $30^\circ \text{C}$  containing  $20 \text{ g dm}^{-3} \text{ Na}_2\text{H}_2\text{PO}_2 \cdot \text{H}_2\text{O}$ . The film was found to contain 21 at % P by EDX.

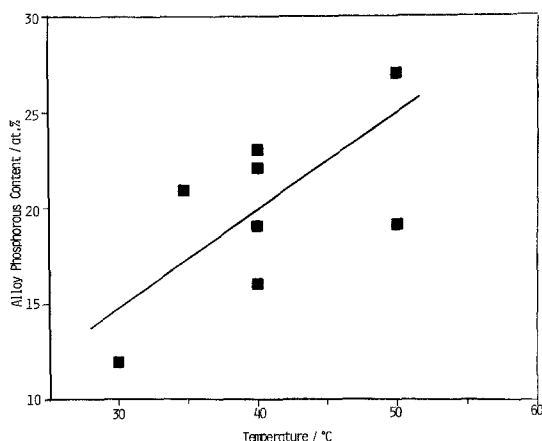


Fig. 4. Alloy phosphorous content against temperature. Experiments were conducted at  $20 \text{ A dm}^{-2}$ . The plating bath fused shown in Table 1 contained  $15 \text{ g dm}^{-3}$  of  $\text{NaH}_2\text{PO}_2 \cdot \text{H}_2\text{O}$ .

direct relationship to the composition of the deposits. The thicknesses of these coatings varied from 2 to  $15 \mu\text{m}$ .

An applied current density of  $25 \text{ A dm}^{-2}$  resulted in 'matted' coatings. The phosphorous content varied from 5 to 17 at % (see Fig. 5), with efficiencies comparable to those obtained at  $20 \text{ A dm}^{-2}$ . There is little compositional effect due to an increase in current density from 20 to  $25 \text{ A dm}^{-2}$ . The compositional difference was much more pronounced when the current density was increased from 15 to  $20 \text{ A dm}^{-2}$ .

A metallic coating could not be obtained at a current density of  $30 \text{ A dm}^{-2}$ . A deep greenish film, probably a chromium hydroxide precipitate, resulted which could be easily scraped off the substrate.

The data show that for a given bath composition, an increase in the current density generally results in a corresponding decrease in the P content (Fig. 5). This is explained as follows. As compared to Cr, P deposition takes place (on thermodynamic basis) at more positive potentials hence an increase in the current density would result in higher rates of Cr(III) reduction. The influence of varying the current density from 20 to  $25 \text{ A dm}^{-2}$  on alloy composition is not as distinguishable as it is by changing the current from 15

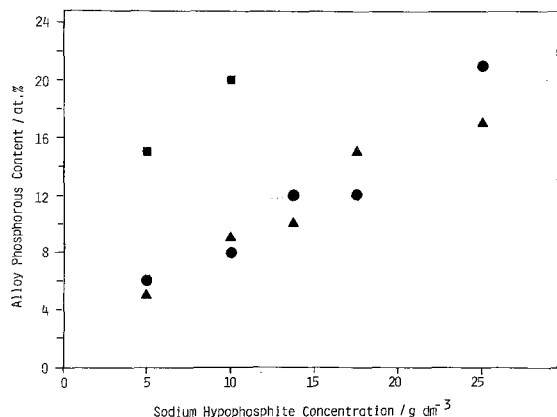


Fig. 5. Alloy phosphorous content against applied current density and the bath phosphorous concentration. Electrodeposition was carried out from the plating bath shown in Table 1 at  $30^\circ\text{C}$ . C.d.: (■) 15, (●) 20 and (▲)  $25 \text{ A dm}^{-2}$ .

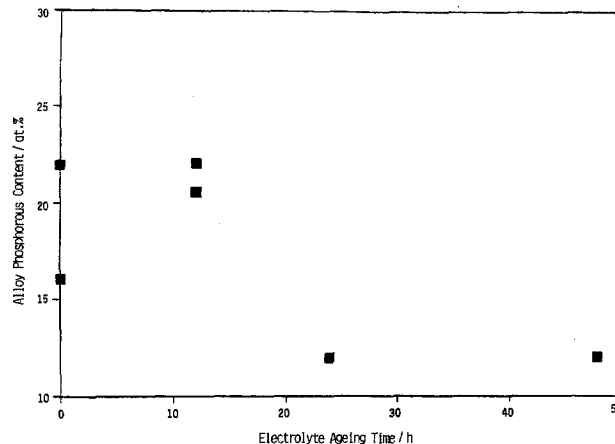


Fig. 6. Alloy phosphorous content against bath ageing time. Plating was carried out at  $40^\circ\text{C}$  and  $20 \text{ A dm}^{-2}$  using the bath shown in Table 1 ( $15 \text{ g dm}^{-3}$   $\text{Na}_2\text{H}_2\text{PO}_2 \cdot \text{H}_2\text{O}$ ).

to  $20\text{--}25 \text{ A dm}^{-2}$ . We speculate that at high current densities, in addition to phosphorous deposition being mass transport limited, the chromium deposition is also partially mass transport controlled. Thus, the influence of increasing the current density on the alloy composition at high rates ( $20\text{--}25 \text{ A dm}^{-2}$ ) is small. We would also like to draw the attention of the reader to the method of analysis used for the determination of elemental composition (i.e. EDX) which is not very sensitive to small difference in composition.

### 3.5. Effect of electrolyte ageing and additives

The influence of electrolyte ageing on the deposit composition was also investigated. Plating was carried out at  $40^\circ\text{C}$  and  $20 \text{ A dm}^{-2}$  using the bath composition shown in Table 1 ( $15 \text{ g dm}^{-3}$   $\text{NaH}_2\text{PO}_2$ ). The data show that freshly prepared baths have higher metalloid content than the ones that have been aged for 10 h and more (Fig. 6). For example, about 22 at % phosphorous was observed in a deposit prepared from an unaged bath as compared to about 11 at % phosphorous content in a deposit prepared from the bath that was allowed to age for 24 h. The influence of various additives on deposition characteristics was also studied and the results obtained are shown in Table 2. When ammonium sulphate was not added to the plating bath, the phosphorous content of the deposit was observed to increase while the coulometric efficiency decreased sharply. The cell voltage needed to maintain the desired current density ( $20 \text{ A dm}^{-2}$ ) was found to increase sharply to  $\approx 14\text{--}15 \text{ V}$  as compared to about 9 V needed for deposition when bath shown in Table 1 was used. Thus, in addition to acting as a complexant possibly in the high pH of the diffusion layer, we also believe that  $(\text{NH}_4)_2\text{SO}_4$  enhances the bath conductivity significantly. Again, when  $\text{NH}_4\text{Br}$  was not present in the bath, the coulometric efficiency declined sharply. In the absence of  $(\text{NH}_4)_2\text{SO}_4$  and  $\text{NH}_4\text{Br}$ , the deposits obtained were nonuniform and of poor quality.

The alloy deposition rate as a function of the time of deposition was also determined. Experiments were conducted at  $35^\circ\text{C}$  and  $20 \text{ A dm}^{-2}$  using the plating

Table 2. The influence of various additives on deposition characteristics. Experiments carried out at 40°C and 20 A dm<sup>-2</sup>. 15 g dm<sup>-3</sup> of Na<sub>2</sub>H<sub>2</sub>PO<sub>2</sub> used in the plating bath.

Bath	Cell voltage/V	Phosphorous content/at %	Coulometric efficiency/%	Deposit quality†
1. As in Table 1	≈ 9	16.02; 23.15; 22.37	7.12; 6.79; 3.72	homogeneous, bright
2. No (HN <sub>4</sub> ) <sub>2</sub> SO <sub>4</sub>	≈ 14–15	26.20	1.45	not uniform
3. No NH <sub>4</sub> Br*	≈ 9–10	24.00	1.25	not uniform; "streaky" surface

\* Otherwise the bath composition as in Table 1

† Visual observation

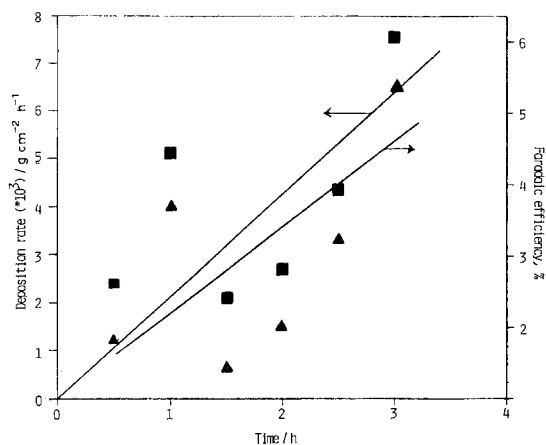


Fig. 7. Alloy deposition rate against plating time. (■) Deposition rate; (▲) efficiency. Plating was carried out at 35°C and 20 A dm<sup>-2</sup> using the bath shown in Table 1 (15 g dm<sup>-3</sup> Na<sub>2</sub>H<sub>2</sub>PO<sub>2</sub> · H<sub>2</sub>O).

bath shown in Table 1 (15 g dm<sup>-3</sup> NaH<sub>2</sub>PO<sub>2</sub>). The deposition rate expressed in g cm<sup>-2</sup> h<sup>-1</sup> is observed to increase with the time of reaction (Fig. 7). It is also interesting to note that although the coulometric efficiencies are low, they also increase with the time of reaction. The data suggest that the Cr-P alloy acts as a better substrate than the Cu discs used for alloy deposition in our experiments.

### 3.6. Structure of electrodeposits

All of the alloys that were analysed by XRD were found to be amorphous. In a related study, DeNeve [23], using transmission electron microscopy, has shown the deposits to consist entirely of an amorphous phase. A more detailed analysis of the physical properties of the electrodeposits will be reported at a later date. The diffraction pattern of an alloy prepared at 25 A dm<sup>-2</sup> and 30°C (5 at % P) is given in Fig. 8. The broad Gaussian peak at an angle of approximately 43° indicates the alloy is amorphous. The chromium-carbon alloy was also found amorphous by XRD. The diffraction pattern of a conventional chromium electrode is also shown in Fig. 8. Bright chromium plate is strongly grain-oriented, with the (1 1 1) plane parallel to the basic metal (2 2 4). This preferred orientation was observed to persist after recrystallization (2 2 2).

### 3.7. Cyclic voltammetry studies

Figure 9 is a cyclic voltammogram for the deposition of the chromium alloy from the chromium-phosphorus-carbon plating bath utilized for alloy deposition, on a glassy carbon microelectrode. The potential scan in the negative direction resulted in a

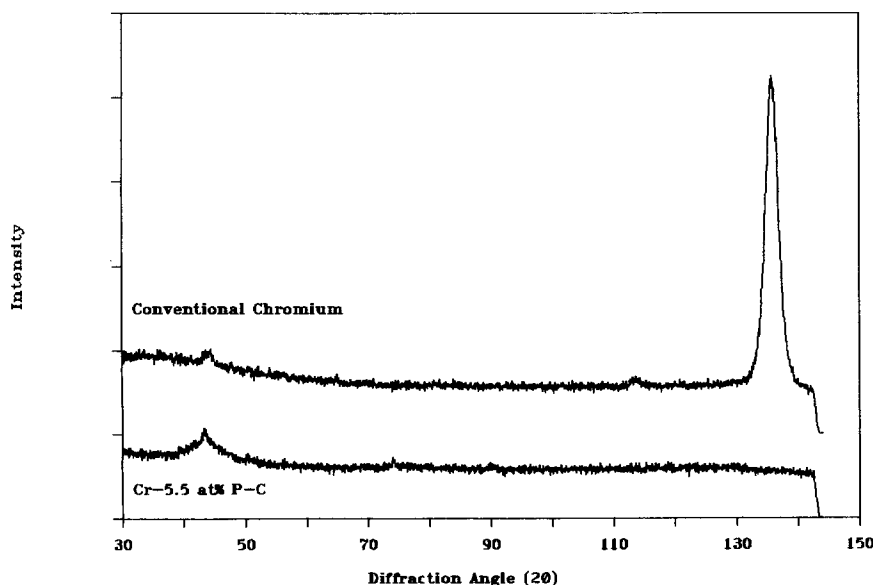


Fig. 8. X-ray diffraction pattern for Cr-5 at % P-C alloy prepared at 25 A dm<sup>-2</sup> and 30°C.

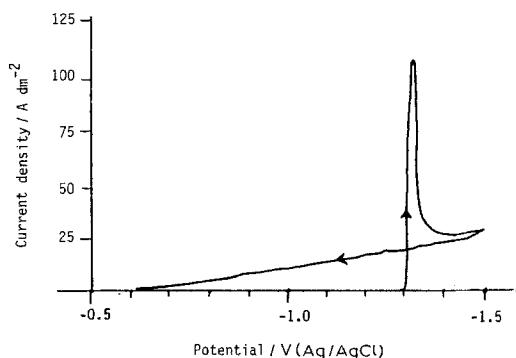


Fig. 9. Cyclic voltammetry on glassy carbon electrode at  $100 \text{ mV s}^{-1}$ . Bath composition as in Table I ( $15 \text{ g dm}^{-3} \text{ Na}_2\text{H}_2\text{PO}_2 \cdot \text{H}_2\text{O}$ ).

pronounced sharp peak at  $-1.31 \text{ V}$  against  $\text{Ag/AgCl}$ . This peak corresponds to the potential necessary for nucleation of the chromium alloy on the glassy carbon surface. The peak current corresponding to this potential is  $9.2 \times 10^{-2} \text{ A}$  with a scan rate of  $100 \text{ mV s}^{-1}$ . The standard redox potential for the  $\text{Cr(III)/Cr}$  reaction is  $-1.03 \text{ V}$  against  $\text{Ag/AgCl}$ . When the electrode was scanned to  $-1.5 \text{ V}$  against  $\text{Ag/AgCl}$ , the resulting current density was found to be approximately  $25 \text{ A dm}^{-2}$ . This is in the current density range used for alloy deposition on the copper substrate in this work.

On the reverse scan in the positive direction, the current remains cathodic, but decreases as the applied potential becomes more positive. Very small anodic currents, on the order of  $10^{-5} \text{ A}$ , were measured at potentials more positive than  $-0.15 \text{ V}$  against  $\text{Ag/AgCl}$ , but no pronounced peaks corresponding to the oxidation of the alloy were apparent, even up to a potential of  $0 \text{ V}$  against  $\text{Ag/AgCl}$ . This indicates that the electrodeposited alloy is resistant to stripping. This behaviour is similar to that observed by Howarth and Pletcher [24] for  $\text{Cr(III)}$  deposition.

Cyclic voltammetry was performed with the plating bath used in this study, without the phosphorus and carbon-containing components. With a scan rate of  $100 \text{ mV s}^{-1}$ , the nucleation potential occurred at  $-1.32 \text{ V}$  against  $\text{Ag/AgCl}$ , with a peak current of  $4.5 \times 10^{-2} \text{ A}$ , which is half of that obtained when the chromium complexant was present. Although in our experiments, there was not significant shift in the deposition potential due to the presence of formic acid and sodium hypophosphite, the high deposition currents observed in solutions containing formic acid lead us to speculate that it may act as a ligand for  $\text{Cr(III)}$ . However, it is also known that ideally the ligand should also catalyse the metal ion reduction and several sulphur ligands which adsorb on the surface of metals, which are known to reduce the overpotential of  $\text{Cr(III)}$  reduction [24–27].

#### 4. Conclusions

A new bath for electrodeposition of amorphous  $\text{Cr-P}$  thin films has been developed and tested. The alloys

were electroplated from a trivalent chromium salt, with sodium hypophosphite as the phosphorous source and formic acid as the chromium complexant and the source of metalloid. The alloys were found to be amorphous by XRD spectroscopy. The phosphorous content of the alloys could be controlled by varying the sodium hypophosphite concentration in the bath, current density, and temperature.

#### Acknowledgements

This research was supported by a grant from the Materials Technology Center, Southern Illinois University, Carbondale, IL 62901. Useful discussions about this research were held with Prof. J. H. Swisher.

#### References

- [1] H. H. Liebermann and N. DeCristofaro, Technology of Amorphous Alloys, in *Chemtech*, June (1987) 363–7.
- [2] J. K. Dennis and T. E. Such, 'Nickel and Chromium Plating', Butterworth, London (1972) p. 186.
- [3] *Idem, ibid.*, p. 184.
- [4] J. P. Hoare, *Plat. Surf. Finish.*, Sept. (1989) 46–52.
- [5] D. Smart, T. E. Such and S. J. Wake, *Trans. Inst. Met. Finish.* **61** (1983) 105–10.
- [6] T. Yoshida, VSP Z, 704, 273 (Patent applied for 28/9151).
- [7] T. Ishiguro, *J. Electrochem. Soc. (Japan)* **23** (1955).
- [8] J. C. Crowther and S. Renton, *Electroplat. & Met. Finish.* **28** (1975), 6–14.
- [9] A. Hoshino, H. A. Laitinen and G. B. Hoflund, *J. Electrochem. Soc.* **133** (1986) 681–5.
- [10] G. B. Hoflund, D. A. Asbury, S. J. Babb, A. L. Grogan, H. A. Laitinen and S. Hoshino, *J. Vac. Sci. Technol.*, **A4**(1), (1986) 26–30.
- [11] G. B. Hoflund, A. L. Grogan, D. A. Asbury, H. A. Laitinen and S. Hoshino, *Appl. Surf. Sci.* **28** (1987) 224–34.
- [12] A. M. Kasaaian and J. Dash, *Plat. Surf. Finish.* **71** (1984) 66–74.
- [13] P. Benaben, *Plat. Surf. Finish.* **76** (1989) 60–3.
- [14] H. Furuya, N. Hasegawa, T. Watanabe and Y. Tanabe, On Amorphous Cr and Amorphous Cr Binary Alloys Prepared by Electroplating Method, in Proceedings of the Fourth International Conference on Rapidly Quenched Metals, Vol. 1, (1981) pp. 93–6.
- [15] M. Takaya, M. Matsunaga and T. Otaka, *Plat. Surf. Finish.* **74** (1987) 70–2.
- [16] I. Drela, J. Szykarczuk and J. Kubicki, *J. Appl. Electrochem.* **19** (1989) 933–6.
- [17] D. J. Willis and C. Hammond, *Mater. Sci. & Technol. (GB)* **2** (June) (1986) 630–6.
- [18] V. V. Bondar and I. I. Potapov, *Zashchita Metallov*, **5**(3) May/June (1969) 346–8.
- [19] A. Watson, M. H. Anderson, M. R. El-Sharif and C. U. Chisholm, *Trans. Inst. Met. Finish* **68** (1990) 26–32.
- [20] M. R. El-Sharif, A. Watson and C. U. Chisholm, *ibid.* **66** (1988) 34–41.
- [21] *Idem, ibid.* **64** (1986) 149–53.
- [22] T. P. Moffat, R. M. Latanision and R. R. Ruf, *Mater. Sci. Eng.* **99** (1986) 525–8.
- [23] B. DeNeve, M.S. thesis, 'Characterization of Amorphous Cr Alloys', Department of Mechanical Engineering and Energy Processes, Southern Illinois University, Carbondale IL, Sept. (1990).
- [24] J. N. Howarth and D. Pletcher, *J. Appl. Electrochem.* **18** (1988) 644–52.
- [25] D. Smart, T. E. Such and S. J. Wake, *Trans. Inst. Met. Finish.* **61** (1983) 105.
- [26] M. J. Weaver, *Israel J. Chem.* **18** (1979) 35.
- [27] N. R. Sorensen, R. B. Diegle and S. T. Picraux, *Corrosion* **43** (1987) 2–7.